Self-similarity and scaling in forest communities

Filippo Simini[a], Tommaso Anfodillo[b], Marco Carrer[b], Jayanth R. Banavar[c,1], and Amos Maritan[a,1]

[a]Dipartimento di Fisica "G. Galilei," Università di Padova, Consorzio Nazionale Interuniversitario per le Scienze Fisiche della Materia and Istituto Nazionale di Fisica Nucleare, via Marzolo 8, 35131 Padua, Italy; [b]Dipartimento Territorio e Sistemi Agro-Forestali, Università di Padova, Agripolis, viale dell'Università 16, 35020 Legnaro (PD), Italy; and [c]Department of Physics, Pennsylvania State University, 104 Davey Laboratory, University Park, PA 16802

Ecological communities exhibit pervasive patterns and interrelationships between size, abundance, and the availability of resources. We use scaling ideas to develop a unified, model-independent framework for understanding the distribution of tree sizes, their energy use, and spatial distribution in tropical forests. We demonstrate that the scaling of the tree crown at the individual level drives the forest structure when resources are fully used. Our predictions match perfectly with the scaling behavior of an exactly solvable self-similar model of a forest and are in good accord with empirical data. The range, over which pure power law behavior is observed, depends on the available amount of resources. The scaling framework can be used for assessing the effects of natural and anthropogenic disturbances on ecosystem structure and functionality.

distribution of tree sizes | energy equivalence principle | finite size scaling | metabolic efficiency | tree shape

Understanding the interrelationships between patterns of size, abundance, and resource availability in tree-dominated communities has proved to be a daunting challenge (1–23). Power law patterns are ubiquitous in plant communities but they are only observed up to a characteristic scale. For example, tree-size distributions in tropical forests scale as a pure power law only when trees smaller than approximately 30–40 cm in diameter are considered and there are fewer larger trees than predicted by a simple power law relationship, (2, 4, 6, 9, 11–16, 18–24). Recent comparative studies (20, 21) of the predictions of metabolic ecology (4, 6, 7, 9, 12, 14, 15, 18, 19, 22, 23) and demographic equilibrium theory (16, 17, 21) suggest the absence of a unique scaling relationship between tree abundance and size in tropical forests across the world. We demonstrate that one can use scaling (25–29) to disentangle universal power law behavior from community dependent detail. We show that scaling yields a model-independent description of ecological communities subject to resource limitations. We apply this general framework to the tree community in the Barro Colorado Island (BCI) forest (24) and show how scaling predicts relationships between ecological quantities in good accord with empirical data. Our predictions match perfectly with the scaling behavior of an exactly solvable self-similar model of a forest. While some of our results are in agreement with earlier work of Brown, Enquist, and West (4, 6, 7, 9, 12, 14, 15, 18, 19, 22, 23), others differ from earlier expectations. Our scaling analysis allows one to analyze situations in which one does not have pure power law behavior, determine the range over which power law behavior is present, and estimate the exponents.

As in earlier work (e.g., refs. 22 and 23 and references therein), we assume that the forest is in steady state and we do not consider the distinction between different tree species. We base our derivations on the following four hypotheses, of which the first two concern a single tree whereas the last two pertain to the whole forest:

1. Tree shape: For a tree of height h, the transverse extension or crown radius is *postulated* to scale as $r_{cro} \sim h^H$. Thus, the crown volume scales as h^{1+2H}. Quite generally, $H \leq 1$. $H = 1$ would imply an isometric tree shape, whereas $H < 1$ would result in a taller tree being more elongated than a smaller one. The scaling analysis predicts the dependencies of various exponents characterizing the *individual tree and the forest* on this shape exponent H and thus provides links between exponents.

2. Energy optimization of a tree: The metabolic rate—mass relationship is obtainable by *maximizing the metabolic rate*, B, for a given tree mass, M. In agreement with empirical data, the metabolic rate, B, of a tree is assumed to be proportional to the number of leaves or to the tree crown volume, $B \sim h^{1+2H}$. This optimization is performed under the hypothesis that the average volume flow rate to the leaves is mass independent [†] (30).

3. Energy optimization of the forest: In order to *maximize the energy utilized by the forest, the leaves must fill the volume of the forest*, which is proportional to the product of the forest area, A, [or equivalently the total number of trees in the forest (10)] and the typical height of the tallest trees (we denote this by h_c). We show below that this allows one to deduce that the tree height probability distribution function (PDF), $p_h(h)$, of a forest is a power law, when $h < h_c$, characterized by an exponent that depends on H.

4. Scaling: We generalize the pure power law behavior that we will deduce from the previous hypotheses building on the finite size scaling approach (25–29). The power of the scaling framework is that it will allow us to carry out a collapse (*SI Text*) to deduce the range of parameters over which pure power law behavior holds and determine the exponents. We consider a scaling form for the fraction of trees with height between h and $h + dh$, given the typical height of the tallest trees in the forest is h_c, $p_h(h|h_c)dh = h^{-\alpha}f_h(h/h_c)dh$ (*SI Text*), where α is the familiar power law exponent. h_c, as shown below, is a measure of the average resource use per tree or equivalently per unit area. The scaling function $f_h(h/h_c)$ is postulated to tend to a constant value when $h \ll h_c$, thus leading to pure power behavior, $p_h(h|h_c) \sim h^{-\alpha}$, and approaches zero when h approaches h_c from below or is greater than it.

The scaling theory, based on the last hypothesis, thus takes into account the resource limitation in an ecological community, which cuts off pure power law behavior. While all scaling relationships involve a power law portion, the presence of the scaling function and the inherent characteristic height arising from resource limitations typically result in the power law behavior occurring over a limited range of scales.

Results

We now proceed to deduce power law exponents and to a verification of the validity of finite size scaling (28, 29) with the available data from the BCI forest (24).

There are at least two distinct masses that one may attribute to a tree: The first is the mass of the fluid contained within the transportation network (i.e., the sapwood) and the second is the total tree mass including also the heartwood (which provides structural stability). The former mass is, of course, contained in the latter. We will assume, for simplicity, that the two masses scales isometrically, i.e., they are proportional to each other. Based on a general theorem pertaining to transportation networks (5), the maximum metabolic rate for a tree of mass M is given by $B \sim M/h$ yielding $M \sim h^{2+2H}$ on using hypothesis 2. This result follows from the observation that efficient directed transport along the tree ensures that the mean distance from the source to all the leaves scales as h. Thus the metabolic rate–mass relationship takes the form $B \sim M^{(1+2H)/(2+2H)}$. We use the same optimization principle of maximizing the metabolic rate for a given mass to deduce that the optimal tree shape is characterized by $H = 1$, yielding the maximum value of the metabolic rate–mass exponent $(1 + 2H)/(2 + 2H)$ of 3/4. This optimal case yields the classic Kleiber law (1, 2), $B \sim M^{3/4}$. Thus in the optimal case, $B \sim h^3$ and $M \sim h^4$. The total tree mass scales isometrically with the mass of the stem (14) and therefore $M \sim r^2 h$, where r is the stem diameter. Thus $r \sim h^{3/2}$, coinciding with the result obtained from considerations of buckling (1). This result justifies the simplifying assumption made above of the isometric scaling of the two distinct definitions of tree mass M. This relationship between tree diameter and height predicts the tapering of the tree trunk and leads to the pleasing result that the metabolic rate $B \sim r^2$ as empirically demonstrated (11).

From allometric theory (1, 2), the characteristic biological time scales as M/B. It is the length of time required for a nonfeeding animal to exhaust its stored metabolic energy or for blood circulation to take place in an organism. Thus, the characteristic mortality rate is predicted to be proportional to B/M and scales as $h^{-1} \sim M^{-1/4} \sim r^{-2/3}$, which is in accord with the empirical data presented by Enquist et al. (22) when $H = 1$. A refinement of the previous argument (*SI Text*) allows one to bridge metabolic ecology (4, 6, 7, 9, 12, 14, 15, 18, 19, 22, 23) with demographic equilibrium theory (16, 17, 21).

To summarize, we have used a single optimization principle of maximizing the metabolic rate for a given mass to derive the shape and energy intake of a tree. Now, we utilize the same principle at the level of a forest, i.e. hypothesis 3, to determine the forest structure.

Let us first assume, consistent with hypothesis 4, that the PDF of the tree heights, $p_h(h)$, is zero both below some recruitment height, h_0, (lower cutoff) and above the typical height of the tallest tree, h_c, (upper cutoff) with $h_c \gg h_0$. Using hypothesis 3, the total energy utilized by the whole forest is given by the alternative expressions in the two sides of the following equation:

$$A h_c = A \int_{h_0}^{h_c} dh\, p_h(h) h^{1+2H}. \qquad [1]$$

Ah_c is the total volume at disposal of the forest whereas $A dh p_h(h)$ is the total number of trees with heights in the interval $(h, h + dh)$. Thus $A dh p_h(h) h^{1+2H}$ is the metabolic rate of (or volume occupied by) trees with their heights in that range. If $p_h(h)$ is a continuous function, the above equation readily implies that

$$p_h(h) \stackrel{H=1}{\propto} h^{-3}\Theta(1 - h/h_c), \qquad h > h_0 \qquad [2]$$

where the Θ function is 1 if the argument is positive and zero otherwise. The distribution of stem radii follows from the

Table 1. Scaling relationships for tropical forests. Summary of the key predictions of the idealized scaling framework. The second row shows the exponent ω characterizing the scaling relationships of the form $y \sim x^\omega$, where x is the tree height h and $y = h, r, r_{cro}, \ldots$. The third row presents the ω values for the idealized case of $H = 1$. Our analysis predicts that the PDF of y satisfies the scaling form $p_y(y|y_c) = y^{-\alpha} f_y(y/y_c)$ where $y_c \sim h_c^\omega$ and f_y is a suitable scaling function as explained in the Supporting Information. The corresponding value of the exponent α is predicted to be equal to $1 + 2H/\omega$. As an example, the PDF of the distribution of the metabolic rate B is predicted to be

$$p_B(B|h_c) = B^{-\frac{1+4H}{1+2H}} f_B(B/h_c^{1+2H})|_{H=1} = B^{-\frac{5}{3}} f_B(B/h_c^3).$$

	h	r	r_{cro}	r_i	d_s	B	M
ω	1	$\frac{1+2H}{2}$	H	H	$\frac{1+6H}{4}$	$1 + 2H$	$2(1 + H)$
$\omega\|_{H=1}$	1	3/2	1	1	7/4	3	4
α	$1 + 2H$	$\frac{1+6H}{1+2H}$	3	3	$\frac{1+14H}{1+6H}$	$\frac{1+4H}{1+2H}$	$\frac{1+2H}{1+H}$
$\alpha\|_{H=1}$	3	7/3	3	3	15/7	5/3	3/2

relationship between r and h to be $p_r(r) \propto r^{-7/3}\Theta(1 - r/r_c)$ with the cutoff value $r_c \sim h_c^{3/2}$. The case for generic H is reported in Table 1 as well as the exponent values for the distribution of the crown height, the metabolic rate, the plant mass and other attributes using the standard rule for the change of variables. The scaling form postulated in hypothesis 4 for the tree height PDF (and the derived ones for other related variables) follows on substituting $\Theta(1 - h/h_c)$ with a more general function $f_h(h/h_c)$.

The energy equivalence principle states that when trees are binned in discrete size classes, the total energy consumed within each class is the same. We find that this does hold when the size classes are based on tree height (*SI Text*) and not on tree radius as has been suggested previously (9, 22, 23). The characteristic
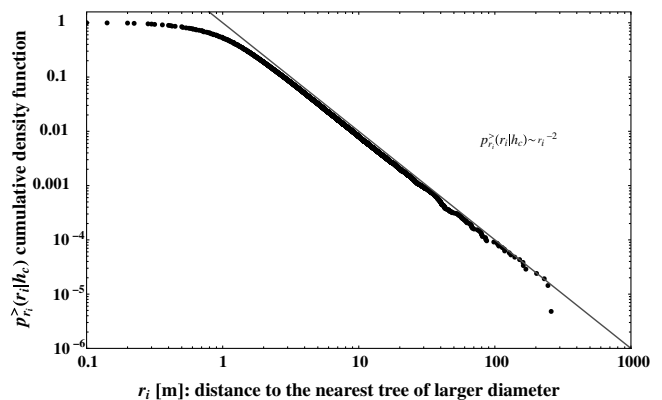
Fig. 1. Cumulative probability distribution of the range of influence r_i for the BCI dataset (1995) (24). $p_{r_i}^>(r_i)$ is the fraction of trees whose minimum distance to a tree of bigger size is $>r_i$ (measured in meters). The solid line is a power law with exponent −2, equivalent to an exponent of −3 for the PDF. Surprisingly, the power law behavior holds up to the size of the forest that is much larger than the largest crown size and there is little need for the scaling function to provide the expected cutoff of pure power law behavior. This fact and that this exponent is independent of H has a simple interpretation. Indeed by assuming a random distribution of trees within the forest, which ought to be true for trees separated by a large distance, one can prove that the PDF of r_i is a power law with the same decay exponent of 3. It is this harmonious matching of exponent values at short length scales (where the tree shape and the width of the crown matter) and the long length scale behavior (where one may apply random distribution considerations), which leads to an almost perfect power law relationship extending over a wide range of r_i.

height of trees, h_c, is a measure of the average energy use per unit area or equivalently per tree. To summarize, we have used the same optimization principle at the tree level and at the forest level of maximizing the metabolic efficiency to derive relationships between, and the values of, exponents characterizing individual tree shape and forest structure. For the forest, the power law behavior of the distribution of tree heights or diameters is derived and not assumed a priori. However the range over which pure power law behavior is observed is limited. We turn now to the issue of how, in practice, one might determine the range over which pure power law behavior holds and estimate the values of exponents.

We begin by introducing an additional variable, the range of influence, r_i, defined as the distance from a given tree to the nearest tree having a larger diameter. Trees compete for light mostly with individuals of their size or greater, and so r_i can be considered as the distance to the nearest significant competitor. The PDF of r_i is predicted to be (Table 1)

$$p_{r_i}(r_i|h_c) = r_i^{-3} f_{r_i}(r_i/h_c^H),$$ [3]

with an exponent value of 3 independent of the specific value of H. The cutoff dependence arises because r_i is expected to scale isometrically with r_{cro} due to competition for space, implying $r_i \sim r_{cro} \sim h^H$.

Fig. 1 shows a plot that confirms the above prediction and, surprisingly, the power law behavior holds up to the size of the forest that is much larger than the largest crown size and there is little need for the scaling function to provide the expected cutoff of pure power law behavior. We will utilize an analysis of this quantity, which exhibits pure power law behavior valid over a wide range, to deduce whether scaling holds in the BCI forest. Before we do that, let us ask why the exponent value is 3, independent of H. Assuming a random distribution of trees within the forest, which ought to be true for trees separated by a large distance, one can prove that the PDF of r_i is a power law with the same decay exponent of 3. It is this harmonious matching of exponent values at short length scales (where the tree shape and the width of the crown matter) and the long length scale behavior (where one may apply random distribution considerations), which leads to an almost perfect power law relationship extending over a wide range of r_i.

Fig. 2. (*A*) Scaling collapse plot. The inset shows the probability of having a range of influence $\geq r_i$ for trees with diameter in the interval $(r, r + \delta r)$. We divided the BCI tree-diameter dataset (24) in 1 cm size bins and for each bin we calculated the cumulative distribution of distances from the nearest neighbor tree of larger size $P_{r_i}^{>}(r_i|r)$. These distributions are shown for r ranging between 1.4 and approximately 49.4 cm in the inset. The main figure depicts a scaling collapse plot of the curves shown in the inset. The scaling framework predicts a collapse plot (see main figure) when the cumulative distributions of distances are plotted against the scaling variable $r_i/r^{2/3}$ when one is in the scaling regime. The gray curves in the inset do not collapse and the black curves define the range of tree diameters over which scaling is observed (2.4 to approximately 31.8 cm). (*B*) Comparison of scaling collapses corresponding to $H = 1/2$ (*Left*) and $H = 1$ (*Right*). These distributions are calculated for sets of trees grouped in 1 cm bins of diameter and are shown for r ranging between 1.4 and approximately 49.4 cm. $H = 1$ clearly provides a better collapse of the $P_{r_i}^{>}(r_i|r)$ distributions, allowing one to rule out the exponent value $H = 1/2$. When the scaling function is substantially constant, $H = 1$ leads to $p(r|h_c) \propto 1/r^{7/3}$ whereas $H = 1/2$ yields the prediction $p(r|h_c) \propto 1/r^2$.

We now turn to an application of finite size scaling through a powerful scaling collapse procedure (28, 29). The conditional PDF of r_i, the range of influence, given the stem diameter r, is predicted to be

$$P_{r_i}(r_i|r) = \frac{1}{r_i} F_{r_i}\left(\frac{r_i}{r^{\frac{2H}{1+2H}}}\right). \qquad [4]$$

Eq. **4** represents the probabilistic generalization of the deterministic counterpart $r_i \sim r^{2H/(1+2H)}$. The prefactor $1/r_i$ ensures that the average of r_i scales as $r^{2H/(1+2H)}$ (more generally, the nth moments of r_i scale as $(r^n)^{2H/(1+2H)}$). The prediction from Eq. **4** is that a plot of the cumulative PDF (which incorporates the prefactor on the right hand side) versus $r_i/r^{2H/(1+2H)}$ for various size classes, over which the scaling framework holds, must collapse (28, 29) on to a single plot. Fig. 2 shows the collapse plot of $P_{r_i}(r_i|r)$ for the predicted exponent of $H = 1$. The collapse is optimal for trees with diameters in the range of 2.4–31.8 cm indicating that this is the correct range in which power law behavior ought to be observed and measured. The collapse begins to break down for larger diameters due to resource limitations. The finite size scaling collapse is an objective method for estimating exponents when pure power law behavior is not observed over a significant range of values of the variables being studied leading to a spread of exponent values. Fig. 3 shows the results of two other tests of the consistency of the scaling theory and are compared with previous predictions of metabolic ecology (4, 6, 7, 9, 12, 14, 15, 18, 19, 22, 23). Fig. S1 further demonstrates the validity of our hypothesis.

The scaling framework presented here as well as exponent relationships and exponent values are realized in the self-similar forest model presented below.

The scaling results hold exactly as predicted by our approach for a simple self-similar model that satisfies all the hypotheses. In two (three) dimensions, the forest is represented by a rectangle $L \times h_c$ (a volume $L \times L \times h_c$), where L and h_c represent the linear size of the forest and the height of the tallest trees respectively with $L \gg h_c$. At the zeroth step, we start to fill the ecosystem with the highest trees represented by triangles of height h_c and crown extension h_c with $H = 1$ (upside down pyramids of height h_c and square base $h_c \times h_c$). The area (volume) occupied by a single large
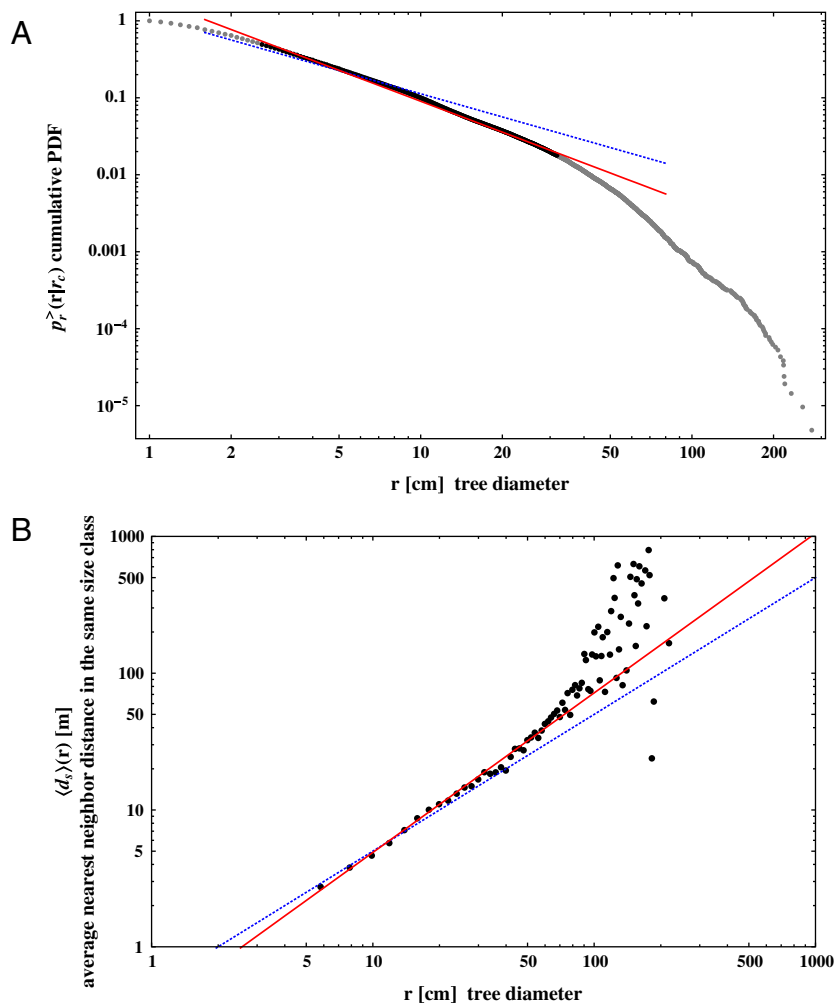
Fig. 3. (A) The cumulative PDF of tree diameters in the BCI forest (1995) (24). $p_r^>(r|r_c)$ is the fraction of trees with diameter $\geq r$. The black dots correspond to diameters in the interval from approximately 2.4–31.8 cm (the range over which scaling is expected to hold from the scaling collapse plot in Fig. 2). The solid line indicates our predicted exponent of $-4/3$ (derived from a power law probability density with exponent $-7/3$). The dashed line depicts the exponent of -1 (corresponding to a probability density with exponent -2) and is shown for comparison. (B) Plot of the average distance from the nearest neighbor individual in the same size class, d_s, versus the tree diameter. We divided the BCI tree-diameter dataset (24) in 2 cm bin size and for each bin, we calculated the average distance between nearest neighbor trees belonging to the same bin. The solid line shows the predicted power law behavior with exponent 7/6, whereas the dashed line is a power law with exponent 1. Our prediction follows from the assumption that the trees in a given size class are distributed uniformly across the forest, thus implying that $d_s \sim P_r(r|r_c)^{-1/2} \sim r^{7/6}$.
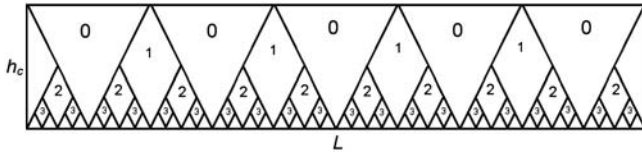
Fig. 4. The two dimensional self-similar forest at step $t = 3$. The lines denote the boundaries of each tree, and the number inside each tree is the time step of its creation. The space without numbers is filled with higher generation trees. Note that it is not crucial to have complete space filling. For example, removing trees at the 0th level does not change the results of our scaling analysis.

tree is a measure of the metabolic rate, $B = h_c^2/2 (B \sim h_c^3)$. The number of the tallest trees is $\rho = L/h_c (\rho = (L/h_c)^2)$. In the next steps—labeled with index $t > 0$—we introduce trees of a different shape: In two dimensions, the tree now has the shape of a rhombus of height $h(t) = h_c/2^{t-1}$ and transverse extension $h_c/2^t$. As shown in Fig. 4, they perfectly fill in the empty spaces between trees in the former levels. (In three dimensions, the shape of the tree is an upside down pyramid with a square base with height $h(t) \sim h_c/2^{t-1}$ and base side $\sim h_c/2^t$. A crown of variable shape is attached to the base so that the space between pyramids of two consecutive levels is completely filled, and each tree occupies the same volume proportional to $h(t)^3$. The three dimensional case is self-similar as well but is harder to visualize).

In two dimensions, the metabolic rate of a tree of level t is $B(t) = (h_c/2^t)^2$ and there are exactly $N(t) = \rho 2^{t-1}$ trees in step t and $N_>(t) = \rho 2^t$ total trees at step t. Thus the total number of trees with metabolic rate larger than B is $N_>(B) = \frac{L(h_c^2/2-B)}{B^{1/2}}$, where $\Theta(x)$ is the step function equal to 1 when $x > 0$ and 0 otherwise. The PDF is given by $p_B(B|h_c) \propto -\frac{d}{dB}N_>(B) \propto \frac{\Theta(h_c^2/2-B)}{B^{3/2}}$, yielding a probability density function of the form $p_B(B|h_c) = B^{-\varphi}f_B(B/h_c^2)$ with a scaling function $f_B(B/h_c^2) \propto \Theta\left[1 - \frac{2B}{h_c^2}\right]$. The cutoff arises because the largest tree in the model has an area and thus a metabolic rate equal to $h_c^2/2$. Thus the power law $p_B(B) \sim B^{-\varphi}$ holds only when $B < h_c^2/2$—the range over which scaling is observed grows as h_c increases. The other PDFs can be found in a similar manner. For example, $p_h(h|h_c) \propto \frac{\Theta(h_c-h)}{h^2}$, which is consistent with the PDF for B because $B \sim h^2$. Note also that trees of the same size are

uniformly distributed, a postulate used to derive the d_s scaling shown in Fig. 3B.

A similar analysis in the realistic three dimensional case yields $p_B(B|h_c) \propto \frac{1}{B^{5/3}}\Theta(1 - \frac{cB}{h_c^3})$, where c is a numerical constant. The exponent value of 5/3 is in accord with the results presented in Table 1. Other scaling laws and PDFs follow in a straightforward manner. Using Hypothesis 2, $B \sim r^2$, the above equation gives for the diameter PDF: $p(r|h_c) \propto 1/r^{7/3}\Theta(1 - cr/h_c^{3/2})$. On introducing more realistic ingredients such as randomness in the plant position and size, one finds that the exponent of the power law is robust and does not change whereas the Θ function becomes a smooth function, $f_r(r/h_c^{3/2})$, with the characteristics described in hypothesis 4.

Discussion

We have demonstrated that scaling (28, 29) provides a powerful framework for the analysis of forest data even in the absence of power law behavior over extended scales and yields predictions in accord with data. We have shown that seemingly distinct patterns are all derivable from a single tree shape exponent, H, thus predicting links between them. The scaling results hold exactly as predicted by our approach for an exactly solvable self-similar model that satisfies all the hypotheses. For tropical forests, we have found that the maximum value of $H = 1$, corresponding to the optimization of tree metabolic rate, provides a good fit to data. Our framework is eminently suited for the study of forests across the globe (when detailed information pertaining to the locations of trees and their diameters, heights, and crown shape become available) to understand the steady-state conditions allowing the maximal use of resources, to elucidate the dependence of the value of the shape exponent on latitude and climate, and to understand the effect of disturbances on forest structure, carbon stock, and sink.

1. Kleiber M (1961) *The Fire of Life: An Introduction to Animal Energetics* (Wiley, New York).
2. Schmidt-Nielsen K (1984) *Scaling* (Cambridge Univ Press, Cambridge).
3. Pacala SW, Canham CD, Silander JA, Jr (1993) Forest models defined by field measurements: I. The design of a northeastern forest simulator. *Can J Forest Res* 23:1980–1988.
4. West GB, Brown JH, Enquist BJ (1997) A general model for the origin of allometric scaling laws in biology. *Science* 276:122–126.
5. Banavar JR, Maritan A, Rinaldo A (1999) Size and form in efficient transportation networks. *Nature* 399:130–132.
6. Enquist BJ, Brown JH, West GB (1998) Allometric scaling of plant energetics and population density. *Nature* 395:163–165.
7. West GB, Brown JH, Enquist BJ (1999) A general model for the structure and allometry of plant vascular systems. *Nature* 400:664–667.
8. Damuth J (2001) Scaling of growth: Plants and animals are not so different. *Proc Natl Acad Sci USA* 98:2113–2114.
9. Enquist BJ, Niklas KJ (2001) Invariant scaling relations across tree-dominated communities. *Nature* 410:655–660.
10. Hubbell SP (2001) *The Unified Neutral Theory of Biodiversity and Biogeography* (Princeton University Press, Princeton).
11. Meinzer FC, Goldstein G, Andrade JL (2001) Regulation of water flux through tropical forest canopy trees: Do universal rules apply?. *Tree Physiol* 21:19–26.
12. Niklas KJ, Enquist BJ (2001) Invariant scaling relationships for interspecific plant biomass production rates and body size. *Proc Natl Acad Sci USA* 98:2922–2927.
13. Allen AP, Brown JH, Gillooly JF (2002) Global biodiversity, biochemical kinetics, and the energetic-equivalence rule. *Science* 297:1545–1548.
14. Enquist BJ (2002) Universal scaling in tree and vascular plant allometry: Toward a general quantitative theory linking plant form and function from cells to ecosystems. *Tree Physiol* 22:1045–1064.
15. Enquist BJ, Niklas KJ (2002) Global allocation rules for patterns of biomass partitioning in seed plants. *Science* 295:1517–1520.
16. Coomes DA, Duncan RP, Allen RB, Truscott J (2003) Disturbances prevent stem size-density distributions in natural forests from following scaling relationships. *Ecol Lett* 6:980–989.
17. Kohyama T, Suzuki E, Partomihardjo T, Yamada T, Kubo T (2003) Tree species differentiation in growth, recruitment and allometry in relation to maximum height in a Bornean mixed dipterocarp forest. *J Ecol* 91:797–806.
18. Niklas KJ, Midgley JJ, Enquist BJ (2003) A general model for mass-growth-density relations across tree-dominated communities. *Evol Ecol Res* 5:459–468.
19. Brown JH, Gillooly JF, Allen AP, Savage VM, West GB (2004) Toward a metabolic theory of ecology. *Ecology* 85:1771–1789.
20. Muller-Landau HC, et al. (2006) Testing metabolic ecology theory for allometric scaling of tree size, growth and mortality in tropical forests. *Ecol Lett* 9:575–588.
21. Muller-Landau HC, et al. (2006) Comparing tropical forest tree size distributions with the predictions of metabolic ecology and equilibrium models. *Ecol Lett* 9:589–602.
22. Enquist BJ, West GB, Brown JH (2009) Extensions and evaluations of a general quantitative theory of forest structure and dynamics. *Proc Natl Acad Sci USA* 106:7046–7051.
23. West GB, Enquist BJ, Brown JH (2009) A general quantitative theory of forest structure and dynamics. *Proc Natl Acad Sci USA* 106:7040–7045.
24. Hubbell SP, Condit R, Foster RB (2005) Barro Colorado Forest Census Plot Data. Available at http://ctfs.si/edu/datasets/bci.
25. Kadanoff LP (1966) Scaling laws for Ising models near Tc. *Physics* 2:263–272.
26. Widom B (1974) The critical point and scaling theory. *Physica* 73:107–118.
27. Wilson KG (1983) The renormalization group and critical phenomena. *Rev Mod Phys* 55:583–600.
28. Fisher ME (1971) *Critical Phenomena* (Academic, New York).
29. Stanley HE (1999) Scaling, universality, and renormalization: Three pillars of modern critical phenomena. *Rev Mod Phys* 71:358–366.
30. Anfodillo T, Carraro V, Carrer M, Fior C, Rossi S (2006) Convergent tapering of xylem conduits in different woody species. *New Phytol* 169:279–290.